

Solar energy incident at the receiver of a solar tower plant, derived from remote sensing: Computation of both DNI and slant path transmittance

Thierry Elias, Didier Ramon, Marie-Agnès Garnero, Laurent Dubus, and Charles Bourdil

Citation: [AIP Conference Proceedings](#) **1850**, 140005 (2017); doi: 10.1063/1.4984513

View online: <http://dx.doi.org/10.1063/1.4984513>

View Table of Contents: <http://aip.scitation.org/toc/apc/1850/1>

Published by the [American Institute of Physics](#)

Articles you may be interested in

[Atmospheric extinction in simulation tools for solar tower plants](#)

AIP Conference Proceedings **1850**, 140011 (2017); 10.1063/1.4984519

[Atmospheric transmission loss in mirror-to-tower slant ranges due to water vapor](#)

AIP Conference Proceedings **1850**, 140010 (2017); 10.1063/1.4984518

[Application of simple all-sky imagers for the estimation of aerosol optical depth](#)

AIP Conference Proceedings **1850**, 140012 (2017); 10.1063/1.4984520

[Applicability of ASHRAE clear-sky model based on solar-radiation measurements in Saudi Arabia](#)

AIP Conference Proceedings **1850**, 140001 (2017); 10.1063/1.4984509

[Short-term forecasting of high resolution local DNI maps with multiple fish-eye cameras in stereoscopic mode](#)

AIP Conference Proceedings **1850**, 140004 (2017); 10.1063/1.4984512

[Measurement of circumsolar ratio in high dust loading regions using a photographic method](#)

AIP Conference Proceedings **1850**, 140003 (2017); 10.1063/1.4984511



SUMMER SALE!

30% OFF
ALL PRINT
PROCEEDINGS!

AIP | Conference Proceedings

ENTER COUPON CODE
SUMMER2017

Solar Energy Incident at the Receiver of a Solar Tower Plant, Derived from Remote Sensing: Computation of both DNI and Slant Path Transmittance

Thierry Elias^{1,a)}, Didier Ramon¹, Marie-Agnès Garnero², Laurent Dubus², Charles Bourdil²

¹ HYGEOS, Euratechnologies, 165 avenue de Bretagne, 59000 Lille, France

² EDF R&D, 6 Quai Watier, 78400 Chatou, France

a) Corresponding author: te@hygeos.com

Abstract. By scattering and absorbing solar radiation, aerosols generate production losses in solar plants. Due to the specific design of solar tower plants, solar radiation is attenuated not only in the atmospheric column but also in the slant path between the heliostats and the receiver. Broadband attenuation by aerosols is estimated in both the column and the slant path for Ouarzazate, Morocco, using spectral measurements of aerosol optical thickness (AOT) collected by AERONET. The proportion of AOT below the tower's height is computed assuming a single uniform aerosol layer of height equal to the boundary layer height computed by ECMWF for the Operational Analysis. The monthly average of the broadband attenuation by aerosols in the slant path was $6.9 \pm 3.0\%$ in August 2012 at Ouarzazate, for 1-km distance between the heliostat and the receiver. The slant path attenuation should be added to almost 40% attenuation along the atmospheric column, with aerosols in an approximate 4.7-km aerosol layer. Also, around 1.5% attenuation is caused by Rayleigh and water vapour in the slant path. The monochromatic-broadband extrapolation is validated by comparing computed and observed direct normal irradiance (DNI). DNI observed around noon varied from more than 1000 W/m^2 to around 400 W/m^2 at Ouarzazate in 2012 because of desert dust plumes transported from North African desert areas.

INTRODUCTION

Aerosols generate production losses in solar plants, by attenuating the incident solar radiation [e.g. 1]. Mostly by scattering but also by absorbing solar radiation, they have a strong impact on Direct Normal Irradiance (DNI) [e.g. 2], and a diminished impact on the Global Horizontal Irradiance. It is consequently very important to correctly model aerosol impact for the bankability of concentrated solar plants [1]. Moreover, the solar radiation collected by a solar tower plant (STP) depends not only on the atmospheric column transmittance governing the DNI, but also on the slant path transmittance between the heliostats and the receiver. The slant path contribution can be significant as aerosols are mostly found close to the ground level, and is increased as the heliostat-receiver distance also increases. This paper proposes a method to evaluate the slant path broadband attenuation caused by aerosols.

Several models propose evaluations of such attenuation, but they roughly take into account the aerosol variability. For example, the DELSOL algorithm [3] proposes 10% slant path attenuation for a default clear day and 25% for a hazy day. This is however unrealistic as the aerosol concentration and nature is highly variable in space and time. It is the reason why, in the climate change context, aerosol optical properties are surveyed on a global scale by satellites and ground-based instrument networks. The AEROSOL ROBOTIC NETWORK (AERONET [4]) achieves appropriate time resolution [e.g. 5] and provides extinction data and its variability with best accuracy.

However aerosol optical properties derived by AERONET are integrated along the atmospheric column while we are interested by aerosols at ground level. We choose to adopt the method proposed by Elias *et al.* [6] who modelled the aerosol vertical distribution by using a layer height characteristic of the main aerosol layer, as also done by other authors [e. g. 7, 8, 9, 10]. As an improvement, Elias *et al.* [6] considered the seasonal change of the atmospheric

layering by using the boundary layer height (BLH) estimated by the European Centre for Medium-range Weather Forecast (ECMWF) for the Operational Analysis. As observed by Skupin *et al.* [9], it is preferable to use a constant value of the layer height during the day.

Also, the computation of the energy loss requires to know the aerosol extinction in the whole solar spectrum, while AERONET and most aerosol-dedicated instruments run in monochromatic modes. The monochromatic-broadband extrapolation is done similarly to Hanrieder *et al.* [11]. However, as only direct transmission is considered, and forward scattering is not accounted for, formally, no radiative transfer code is necessary. The radiative transfer code libraries are sufficient to estimate the column transmittance. The monochromatic-broadband extrapolation is validated by making comparisons between computations from AERONET and independent observations of *DNI*.

The objective of the paper is to compute the mean slant path broadband transmittance and its variability, in realistic conditions, and more specifically the aerosol contribution. Computations are presented for the location of Ouarzazate (Morocco) in August 2012, using: 1) the aerosol optical thickness (AOT) and the atmospheric column water vapour content delivered by AERONET; 2) *BLH* provided by ECMWF for the Operational Analysis, to estimate the proportion of *AOT* below the tower's height [6]. We first present the equations to compute both *DNI* and the slant path transmittance from observed *AOT*, the monochromatic-broadband extrapolation is then validated and the aerosol contribution to the slant path transmittance is presented for August 2012 at Ouarzazate.

EQUATIONS AND THE RADIATIVE TRANSFER APPROACH

Transmittance

The slant path transmittance in the broadband solar spectrum between 290 and 3000 nm [12], $T_{surf}(\Delta\lambda)$, depends on *DNI* and on the spectral characteristics of 1) the solar irradiance $E_{sun}(\lambda)$; 2) the atmospheric column transmittance $T_{col}(\lambda)$; and 3) the slant path transmittance $T_{surf}(\lambda)$:

$$T_{surf}(\Delta\lambda) = \frac{F_{ESD} \int_{250nm}^{4000nm} E_{sun}(\lambda) T_{col}(\lambda) T_{surf}(\lambda) d\lambda}{DNI} \quad (1)$$

F_{ESD} is the Earth-Sun distance correcting factor. *DNI* is defined according to the 'strict' definition given by Blanc *et al.* [12], with the only extinction in the solar direction and no atmospheric scattering from other directions to the solar direction, and therefore no consideration of the circumsolar radiation, as:

$$DNI = F_{ESD} \int_{250nm}^{4000nm} E_{sun}(\lambda) T_{col}(\lambda) d\lambda \quad (2)$$

The monochromatic transmittances can be decomposed as:

$$T_{col}(\lambda) = T_{Ray,col}(\lambda) T_{gas,col}(\lambda) T_{aer,col}(\lambda) \quad (3a)$$

$$T_{surf}(\lambda) = T_{Ray,surf}(\lambda) T_{H2O,surf}(\lambda) T_{aer,surf}(\lambda) \quad (3b)$$

$T_{Ray,col}(\lambda)$ and $T_{Ray,surf}(\lambda)$ are the transmittances caused by Rayleigh scattering, depending on the atmospheric pressure. $T_{gas,col}(\lambda)$ and $T_{H2O,surf}(\lambda)$ are transmittances caused by absorbing gases. Main variable absorbing gases in the atmospheric column are water vapour and ozone, and only water vapour is considered in the slant path. Rayleigh and gas transmittances are computed according to the AFGL US summer standard atmosphere [13], with the column amount of water vapour constrained by the AERONET observation, also providing *AOT*. The monochromatic aerosol transmittance is defined according to the Beer-Lambert-Bouguer law as:

$$T_{aer,col}(\lambda) = e^{-\frac{AOT(\lambda)}{\cos(SZA)}} \quad (4a)$$

$$T_{aer,surf}(\lambda) = e^{-\frac{\Delta AOT(\lambda)}{\cos(SPA)}} \quad (4b)$$

where SZA is the solar zenith angle and SPA the slant path angle (Fig. 1). $\mathcal{A}OT$ is the aerosol optical thickness from ground level up to the receiver's height. Next Section shows how $\mathcal{A}OT$ can be related to AOT as well as to the solar plant and boundary layer dimensions.

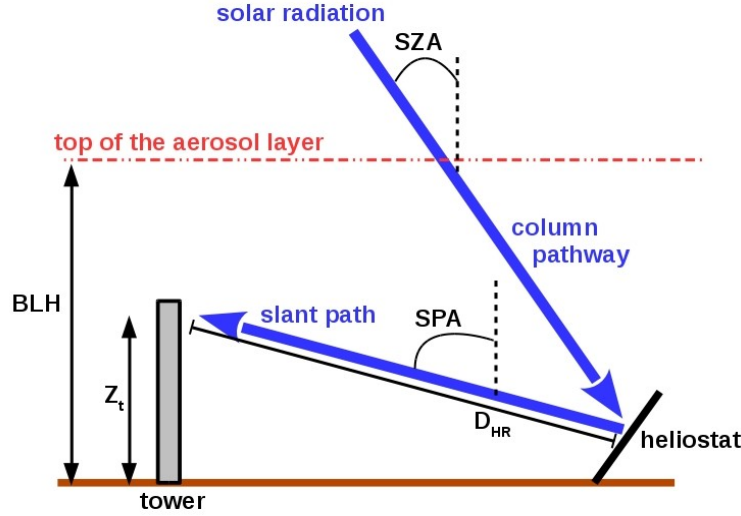


FIGURE 1. Schema of the optical pathway from top of the atmosphere to the receiver at the tower's top. SZA =solar zenith angle, SPA = slant path angle, BLH =boundary layer height, z_t =tower's height, D_{HR} = heliostat-receiver distance.

Aerosol Extinction Coefficient at Ground Level

AOT provided by AERONET is related to the aerosol extinction coefficient (AEC) as:

$$AOT = \int_0^{z_{TOA}} AEC(z) dz \quad (5a)$$

where z is the height above ground level, up to the Top of the Atmosphere (TOA). We get a simplified equation relating $AEC(z=0)$ and AOT , assuming any of two hypothesis about the vertical distribution of aerosols. First hypothesis is a uniform distribution of aerosols in a single aerosol layer [6], with AEC not depending on z , and Eq. 5a becomes:

$$AOT(\lambda) = AEC(\lambda) ALH \quad (5b)$$

where ALH is the aerosol layer height and AEC the constant value for the whole aerosol layer. In the second hypothesis, the aerosol extinction in a single aerosol layer follows an exponential decay in the vertical direction [e.g. 7, 8], at the rate of ALH :

$$AEC(z) = AEC(z = 0) \exp\left(\frac{-z}{ALH}\right) \quad (6)$$

The integration along the vertical [e.g. 7] gives:

$$AOT = \int_0^{z_{TOA}} AEC(z) dz = AEC(z = 0) \int_0^{z_{TOA}} \exp\left(\frac{-z}{ALH}\right) dz = AEC(z = 0) ALH \left(1 - \exp\left(\frac{-z_{TOA}}{ALH}\right)\right) \quad (7)$$

As z_{TOA} , is much larger than ALH , Eq. 7 results in the same expression as for a uniform aerosol layer (Eq. 5b). Consequently, in any of the two hypothesis, ground level AEC can be obtained from AERONET as:

$$AEC(\lambda) = AOT(\lambda) / ALH \quad (8a)$$

Moreover, as done by Elias *et al.* [6], we make the hypothesis that *ALH* is equal to the boundary layer height (*BLH*) provided by ECMWF:

$$AEC(\lambda) = AOT(\lambda) / BLH \quad (8b)$$

Skupin *et al.* [9] showed that ground-based measurements of *AEC* are underestimated in the morning with *BLH* changing with the time of the day, while better agreement is found with a constant layer height. Indeed lidar measurements showed that *BLH* is much smaller than *ALH* during the morning and they become similar from noon. Consequently, as proposed by Elias *et al.* [6], we use the value of *BLH* at 15:00 at Ouarzazate.

Following Eq. 5a, the aerosol optical thickness below the tower's height is defined as:

$$\Delta AOT = \int_0^{z_T} AEC(z) dz \quad (9)$$

with z_T the tower's height (**Fig. 1**). With the hypothesis of a uniform aerosol layer, *AEC* is constant from the heliostat to the receiver:

$$AOT = AEC z_T \quad (10)$$

In the hypothesis of the exponential decrease, *AEC* is only 5-10% smaller at 200 m height than at ground level if *ALH*=2-4 km, and consequently we consider *AEC* is constant, and Eq. 10 is also valid. With Eq. 8b, Eq. 10 becomes:

$$AOT = AOT z_T / BLH \quad (11)$$

and Eq. 4b can be written as:

$$T_{aer,surf}(\lambda) = e^{-\frac{AOT(\lambda) z_T}{\cos(SPA)BLH}} \quad (12)$$

Radiative Transfer Computations

Computations are made for Ouarzazate, Morocco: 30.92837° N, 6.91287° W, 1136 m above sea level. The slant path transmittance is computed for a distance D_{HR} of 1 km between a heliostat and the receiver, giving $SPA=78.7^\circ$ for a tower of 200 m. The slant path transmittance is computed for August 2012, when the monthly average of *BLH* is 4.7±0.3 km at 15:00, according to ECMWF Operational Analysis.

Monochromatic transmittances, from top of the atmosphere to ground level, and from ground level up to the tower's top, are computed according to the Beer-Lambert-Bouguer law (Eq. 4a and 12 for aerosols). Broadband quantities are computed according to Eq. 1 and 2. The Rayleigh optical depth is computed according to Bodhaine *et al.* [14]. Ozone and NO₂ absorption cross sections are taken from Bogumil *et al.* [15], and for other gases like H₂O, CO₂, CH₄, we used the absorption band parametrization called REPTRAN [16] at the resolution of 15 cm⁻¹. The gas and thermodynamic profiles are adopted from the AFGL US summer standard atmosphere [13]. The extraterrestrial solar spectrum is taken from Kurucz [17].

AERONET measurements are used for column water vapour content as well as the aerosol load and type. The water vapour optical thickness computed from the AFGL US summer standard atmosphere is scaled linearly with the column water content provided by AERONET. Then the AFGL US summer profile is used to derive the proportion at surface level. We consider the measured *AOT* spectral dependence, while the empirical models usually computed *DNI* with a constant value of the Ångström exponent, according to Gueymard [2]. We mix desert dust and continental aerosols as modelled by OPAC [18] to reproduce both the aerosol optical thickness and the Ångström exponent measured by AERONET. The resulting model is used to compute the optical thickness at all wavelengths of the solar spectrum. Slant path transmittance is computed at 15-min resolution with 15-min averages of *AOT* but the monthly average of *BLH*.

VALIDATION OF THE MONOCHROMATIC-BROADBAND EXTRAPOLATION

The monochromatic-broadband conversion is validated in the atmospheric column by comparing computed *DNI* with local measurements made at Ouarzazate. The absolute difference in *DNI* between March and September 2012 was 10 W/m^2 with 30 W/m^2 standard deviation. 10 W/m^2 represents 1 to 2.5% of the diurnal maximum, and represents more for increasing *SAZ*. The root mean square difference was 42 W/m^2 for one year at 15-minute resolution, and $0.32 \text{ kWh/m}^2/\text{day}$ for the daily exposure. Figure 2 shows the comparison for several days in function of the Universal Time, with contrasted aerosol loads. All comparisons show that *DNI* is satisfyingly reproduced. Largest differences are caused by heterogeneities in the cloud cover or the aerosol plumes.

On both 28 July and 26 August 2012, *AOT* was fairly constant during the day, but with a factor of 3 in *AOT* between the two days: *AOT* at 500 nm was only 0.06 on 28 July but 0.22 on 26 August. Also the water vapour content was twice larger on 26 August. The sensitivity to *SAZ*, the impacts of both different aerosol load and different water content are all correctly reproduced (Fig. 2).

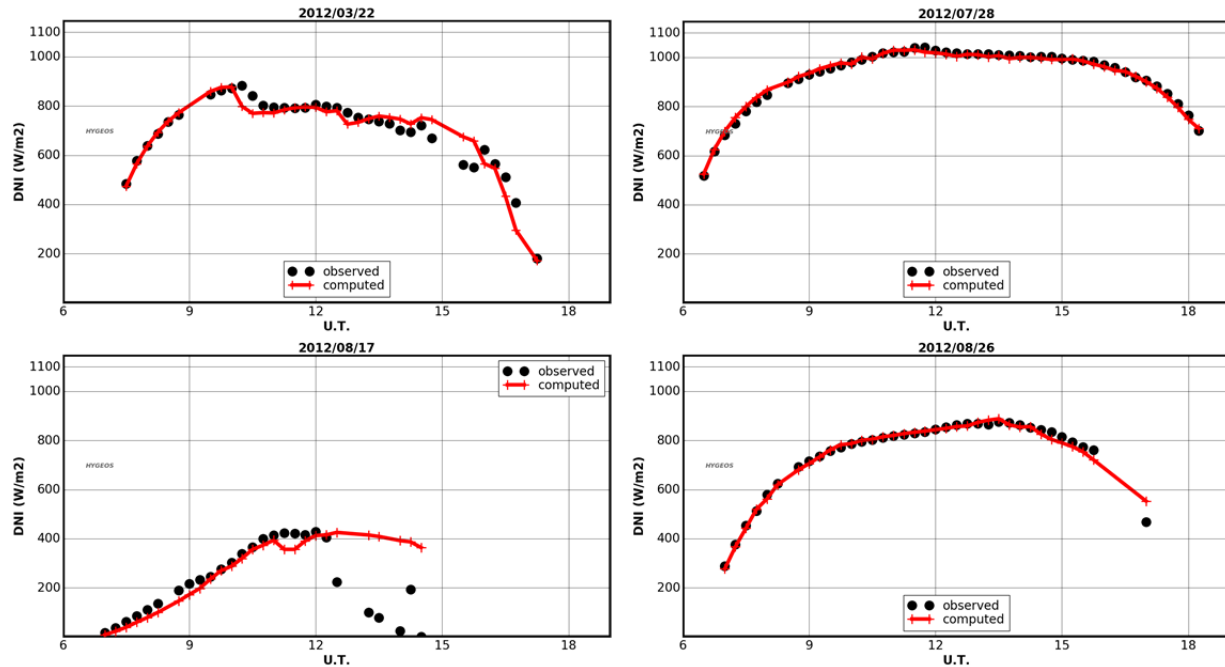


FIGURE 2. Computed and observed *DNI* during 4 days at Ouarzazate. *AOT* is constant during the day for right hand side figures and the standard deviation is 0.10 on 22 March (left top) and 17 August (left bottom).

On 22 March, *AOT* was highly variable, by a factor of 4 from sunset to sunrise. Agreement was good during the morning and the changing impact of *AOT* was correctly computed, even if some time delays could be observed, caused by heterogeneities in the aerosol plume spatial extent. On 17 August, when *AOT* reached the annual maximum at 1.03 ± 0.09 , the agreement was satisfying before noon, even if *DNI* was slightly underestimated. The Ångström exponent was 0.13, typical of desert dust. The change from 28 July to 17 August was similar to what was reported by Gueymard [1]. However, a large disagreement was observed in the afternoon, which was caused by clouds over the pyrheliometer (measuring *DNI*) site, generating values smaller than 200 W/m^2 around 14:00, while AERONET estimates are close to 400 W/m^2 . Measurements were not taken by AERONET after 15:00 and neither on the following day (18/08/2012), showing that the clouds reached the AERONET site few hours later than the pyrheliometer site, causing the differences from noon.

THE SLANT PATH TRANSMITTANCE

The monthly average of the slant path attenuation caused by aerosols was $6.9 \pm 3.0\%$ in August 2012, because of desert dust aerosols. The aerosol optical thickness was 0.36 ± 0.17 and the Ångström exponent was 0.27 ± 0.07 . The

large standard deviation of 3% was caused by changes in the aerosol load, as illustrated by the standard deviation of 0.17 in AOT in only 1 month. Similarly, Hanrieder *et al.* [20] estimated an atmospheric extinction of 7% for the Plataforma Solar de Almería. The slant path attenuation added to the column attenuation of almost 40%, computed with Eq. 2, 3a, and 4a, results in almost half the solar radiation that is attenuated by aerosols in August 2012 at Ouarzazate.

Figure 3 shows the high variability of the broadband slant path attenuation ($1-T_{surf}$) caused by aerosols, from day to day. In August 2012, the slant path attenuation could reach 20% during a few hours (17/08), when AOT was close to 1.0 at 500 nm, and also be smaller than 5% during cleaner days (e.g. 26/08). Similarly, Polo *et al.* [19] refer to values “below 5% for clean atmospheres to around 20% in haziest conditions”.

Rayleigh scattering and water vapour absorption have minor but non negligible influence in the slant path, with around 1.5% attenuation, while around 14% is attenuated by Rayleigh scattering and gas absorption in the atmospheric column in August. Rayleigh and water vapour slant path attenuation shows a diurnal cycle, with maximum at noon. For example on 6 August, attenuation by Rayleigh scattering is 0.8% at noon with $SZA=15^\circ$, and attenuation by water vapour is 1.4%, while each attenuation is 0.4% at 06:00 with $SZA=88^\circ$, and for constant water vapour columnar content of 0.90 cm. The attenuation in the slant path is decreased when the atmospheric column path is increased, because radiation is fully extinguished at some wavelengths in the column, as in the infra red domain. Figure 3 also shows that the cloud cover is small in August at Ouarzazate, as only 17 August afternoon and 18 August data were missing (Fig. 2).

According to AERONET, the radiant exposure incident at the heliostat is 116 kWh/m² in August 2012, and 106.3 kWh/m² incident at the receiver for a 1-km distance, for 186 h of insulation without clouds. Aerosols present in the slant path in August 2012 reduce the available energy by 7.5 kWh/m².

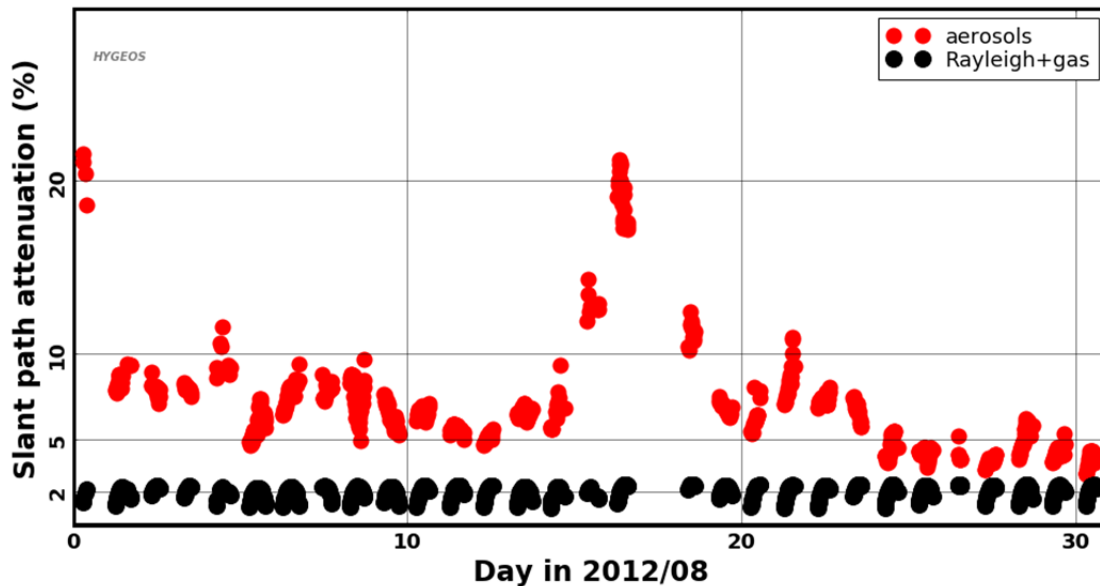


FIGURE 3. The slant path attenuation in the broadband solar spectrum, at Ouarzazate in August 2012, computed with 15-minute AERONET AOT and ECMWF BLH of 4.7 km, for a heliostat-receiver distance of 1 km. Attenuation is showed separately for aerosols (red) and for both Rayleigh scattering and water vapour absorption (black).

Polo and Estalayo [21] showed that the relationship between the incident radiation and the produced energy is not linear, as 7% DNI under-estimation at Sede Boqer resulted in 1% production under-estimation in a STP, and 6% DNI over-estimation resulted in 20% production over-estimation at Tamanrasset. The DNI over-estimation at Tamanrasset was caused by incorrect estimate of high and sudden aerosol loads, which are events also occurring at Ouarzazate. Such events caused such a large attenuation that the STP may not start to work during the entire day [21]. Similarly, Hanrieder *et al.* [20] estimated a range of “losses between 1.6 and 7 % ... considering overload dumping or not”.

By adding the slant path attenuation to the column attenuation, we can consequently expect high impact of aerosols on produced energy at Ouarzazate.

CONCLUSIONS

It is important to consider the aerosol extinction when dealing with solar resource for the solar tower plants. Aerosols scatter and absorb solar radiation in both the atmospheric column and in the slant path between the heliostats and the receiver. Consequently not only *DNI* is reduced because of aerosols but also the slant path transmittance. In average in August 2012 at Ouarzazate, 6.9% of the incident radiation was attenuated by aerosols in the slant path, and further 1.5% by Rayleigh scattering and water vapour absorption. Both clean and hazy DELSOL models would over-estimate the attenuation, and also do not consider the strong aerosol variability.

Transmittance by Rayleigh and water vapour show a diurnal cycle but not the transmittance by aerosols. Indeed both Rayleigh scattering and water vapour absorption are most active in specific wavelengths, and complete extinction may occur at these wavelengths in the column pathway at large solar zenith angles. During this month, aerosols attenuated almost 50% of the solar radiation in both the column and the slant path. The time variability is significant. The slant path attenuation could be smaller than 5% for the clean days and larger than 10% for several days of August 2012. It even reached 20% on 17 August during a severe dust storm.

The only aerosol observation used here is the aerosol optical thickness (AOT) at several wavelengths, performed by AERONET. The proportion of *AOT* from the ground level to the receiver's height is defined following the approach proposed by Elias *et al.* [6], consisting in describing the aerosol vertical profile with the boundary layer height at 15:00, which depends on the season according to ECMWF. The monochromatic-broadband conversion, applied with radiative transfer libraries for aerosols and gases, was validated by making comparisons with independent measurements of *DNI*. The diurnal maximum of *DNI* varied between ~400 and ~1000 W/m² at Ouarzazate in August 2012 because of desert dust. The root mean square difference between computations and measurements was 42 W/m² for one year at 15-minute resolution

AERONET provides the appropriate time resolution for best accuracy [5] but the the data archive may not be long enough when Gueymard [1] advised to consider long time series for assessing the solar plant bankability. Several satellite instruments surveyed the globe for many years and could complement the AERONET network to provide input data to our method.

ACKNOWLEDGEMENTS

The authors are very grateful to the AERONET site operators and instrument owners, and in particular to Taoufik Zaidouni and Emilio Cuevas-Agulló, and to EDF-EN to provide the *DNI* data. The authors also acknowledge ECMWF for providing the boundary layer data.

REFERENCES

1. C. A. Gueymard, [Journal of Solar Energy Engineering, American Society of Mechanical Engineers](#), **133**, 031024, (2011).
2. C. A. Gueymard, [Solar Energy, Elsevier](#), **74**, 355-379 (2003).
3. B. L. Kistler, Technical report, SANDIA (1986), pp. 78.
4. B. N. Holben, T. F. Eck, I. Slutsker, D. Tanré, J. P. Buis, A. Setzer, E. Vermote, J. A. Reagan, Y. Kaufman, T. Nakajima, F. Lavenu, I. Jankowiak, and A. Smirnov, [Rem. Sens. Environ.](#), **66**, 1-16 (1998).
5. M. Schroedter-Homscheidt, and A. Oumbe, [Atmospheric Chemistry and Physics](#), **13**, 3777-3791 (2013).
6. T. Elias, D. Ramon, L. Dubus, C. Bourdil, E. Cuevas-Agulló, T. Zaidouni, and P. Formenti, [AIP Conference Proceedings](#), **1734**, 150004, doi: 10.1063/1.4949236 (2016).
7. J. Qiu, [J. Appl. Meteor.](#), **42**, 1611-1625 (2003).
8. K. H. Lee, M. S. Wong, K. W. Kim, S. S. Park, Analytical approach to estimating aerosol extinction and visibility from satellite observations, [Atmospheric Environment](#), **91**, 127-136 (2014).
9. A. Skupin, A. Ansmann, Engelmann, R., Baars, H. and Müller, T., [Atmospheric Measurement Techniques](#), **7**, 701-712, doi: 10.5194/amt-7-701-2014 (2014).
10. Z. Tahboub, A. Oumbe, Z. Hassar, and A. Obaidli, [Energy Procedia](#), **49**, 2405 - 2413 (2014).
11. N. Hanrieder, S. Wilbert, R. Pitz-Paal, C. Emde, J. Gasteiger, B. Mayer, and J. Polo, [Atmospheric Measurement Techniques](#), **8**, 3467-3480, doi: 10.5194/amt-8-3467-2015, (2015).
12. P. Blanc, Espinar, B., Geuder, N., Gueymard, C., Meyer, R., Pitz-Paal, R., Reinhardt, B., Renné, D., Sengupta, M., Wald, L. and Wilbert, S., [Solar Energy](#), **110**, 561 – 577 (2014).

13. G. Anderson, Clough, S., Kneizys, F., Chetwynd, J., and Shettle, E., Tech. Rep. AFGL-TR-86-0110, Air Force Geophys. Lab., Hanscom Air Force Base, Bedford, Mass. (1986).
14. B. A. Bodhaine, Wood, N. B., Dutton, E. G., and J. R. Slusser, *J. Atm. Ocean Technol.*, **16**, 1854–1861 (1999).
15. K. Bogumil, J. Orphal, Voigt, S., Spietz, P., Fleischmann, O. C., Vogel, A., Hartmann, M., Kromminga, H., Bovensmann, H., and J. P. Burrows, *J. Photochem. and Photobio. A: Chem.*, **157**, 167–184, (2003).
16. J. Gasteiger, C. Emde, B. Mayer, R. Buras, S. A. Buehler, and O. Lemke, *J. of Quantitative Spectroscopy & Radiative Transfer*, **148**, 99-115 (2014).
17. R. Kurucz, Synthetic infrared spectra, in: Proceedings of the 154th Symposium of the International Astronomical Union (IAU); Tucson, Arizona, March 2-6, 1992, Kluwer, Acad., Norwell, MA (1992).
18. M. Hess, P. Koepke, and I. Schult, *Bulletin of the American Meteorological Society*, **79**, 831–844, (1998).
19. J. Polo, J. Ballestrin, and E. Carra, *Solar Energy*, *134*, 219 - 227 (2016).
20. N. Hanrieder, S. Wilbert , M. Schroedter-Homscheidt, F. Schnell , D. Mancera Guevara, R. Buck, S. Giuliano, and R. Pitz-Paal, Solar Paces 2016 (Submitted).
21. J. Polo, and G. Estalayo, *Solar Energy*, **115**, 621 – 631 (2015).